





# Low-frequency Electromagnetic Coupling Between a Traction Line and an Underground Pipeline in a Multilayered Soil

Amauri G. Martins-Britto <sup>\*</sup>, *Member, IEEE*, Caio M. Moraes <sup>†</sup>, *Student Member, IEEE*,  
Felipe V. Lopes <sup>†</sup>, *Senior Member, IEEE*, Sébastien Rondineau <sup>†</sup>, *Senior Member, IEEE*  
Department of Electrical Engineering, University of Brasília, Brasília, Brazil<sup>†</sup>

E-mail: amaurigm@lapse.unb.br<sup>\*</sup>

**Abstract**—This paper presents a low-frequency electromagnetic interference study between a single-phase overhead traction line and a nearby underground pipeline, with emphasis on how the soil structure affects induced voltages. Soil parameters are determined from real field measurements, which results in a soil model composed of six layers. Mutual impedances are computed using the finite element method (FEM) and compared with a modified version of the original Carson equation, in which the term describing the soil conductivity is replaced by a uniform equivalent of the multilayered structure. Results show an excellent agreement between the proposed approach and the reference values, along with a considerable performance gain, compared to the FEM formulation of the multilayer soil structure. In addition, simulations highlight the errors in which one occurs when the soil structure is not properly accounted, especially when the apparent resistivity is used instead of the stratified parameters.

**Keywords**—Electromagnetic interferences, inductive coupling, pipelines, soil resistivity, traction lines.

## I. INTRODUCTION

**T**HE PROBLEM of the mutual electromagnetic interferences (EMI) between transmission lines and other metallic structures is of great importance to those directly or indirectly affected by phenomena dependent on transmission line parameters, such as power companies, engineers in charge of electrical studies and/or designs or pipeline operators which facilities share the right-of-way with energized lines.

Electric traction, which consists of using overhead power lines positioned above railways to provide energy to locomotives, is an efficient and clean solution for modern transportation systems [1]. Moreover, due to the space occupation requirements to operate such systems, electric railroads also provide a convenient pathway for laying out utilities installations, such as pipelines used for gas, water and oil derivatives supply.

An underground pipeline made of conductive material, when exposed to the energized phases of a transmission line, is exposed to a variety of phenomena, which cause the rise of the metal potential along its path, due to the electromotive forces

emerging from the inductive coupling mechanism between the two structures, illustrated in Fig. 1.

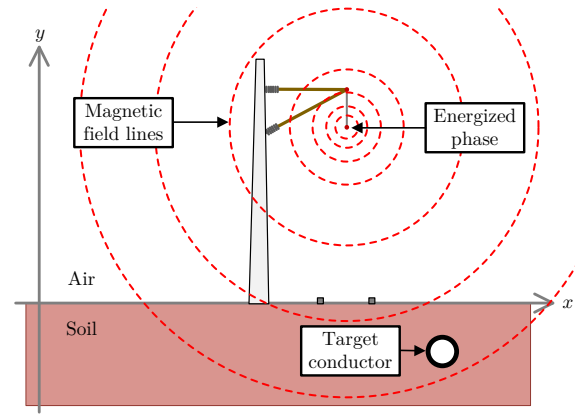


Figure 1: Inductive coupling between an energized phase and a target pipeline.

Induced voltages on the target installation depend on the geometry of the structures, type and arrangement of conductors, current magnitude, type of pipeline coating and soil electrical conductivity, among other factors. These voltages pose risks to the facilities and personnel involved, such as: electrocution caused by touch voltages, insulation breakdown, electrochemical corrosion and damage resulting from current exposure [2]. Thus, the associated safety concerns justify the investment in tools and techniques to predict and mitigate voltages caused by EMI.

Having established the importance of the subject, this work describes an interference study between a traction line and a parallel pipeline considering a soil structure composed of six layers, with parameters determined from actual soil resistivity surveys. Induced voltages are calculated using finite element analysis and a circuit model leveraging a technique recently proposed by the authors, in which the multilayered property of real soils is modeled using the classic Carson equation.

Of practical interest to several power systems applications,

this work is expected to contribute with a demonstration of how to build complex, realistic interference models, using conventional techniques and tools.

## II. MATHEMATICAL MODEL

### A. Induced electromotive forces

Fig. 2 depicts a system composed of a single-phase and a target conductor above a semi-infinite uniform soil.

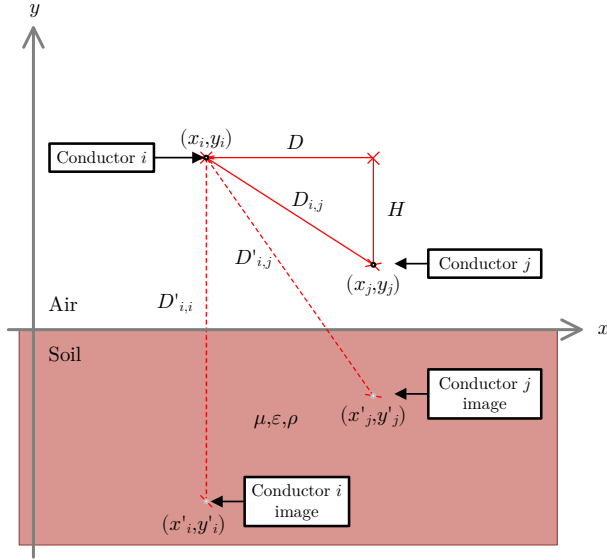


Figure 2: Two conductors above uniform soil.

Assuming harmonic regime with frequency  $f$ , in hertz, if the energized conductor  $i$  carries a current  $I$ , the resulting magnetic field in the vicinities of the exposed conductor  $j$  induces electromotive forces given by (1):

$$E = Z_m \times I, \quad (1)$$

in which  $E$  is the induced electromotive force, given in volts;  $I$  is the source current, in ampères; and  $Z_m$  is the mutual impedance between conductors  $i$  and  $j$  with ground return path, computed in ohms per unit length using Carson equation (2) [3]:

$$Z_m = Z_{i,j} = j\omega \frac{\mu_0}{2\pi} \ln \left( \frac{D'_{i,j}}{D_{i,j}} \right) + j\omega \frac{\mu_0}{2\pi} \int_0^\infty \frac{2e^{-H\lambda}}{\lambda + \sqrt{\lambda^2 + j\omega\mu_0\sigma - \omega^2\mu_0\epsilon_0\epsilon_r}} \cos(\lambda D) d\lambda, \quad (2)$$

in which  $\omega = 2\pi f$  is the angular frequency, in rad/s;  $\mu_0 = 4\pi \times 10^{-7}$  H/m is the free space magnetic permeability;  $\epsilon_0 \approx 8.85 \times 10^{-12}$  F/m is the vacuum electrical permittivity;  $\sigma$  is the soil conductivity, in S/m;  $\epsilon_r$  is the soil relative permittivity;  $H$ ,  $D$ ,  $D_{i,j}$  and  $D'_{i,j}$  are the relative distances represented in Fig. 2, in meters, with:  $H = |y_i - y_j|$ ,  $D = |x_i - x_j|$ ,  $D_{i,j} = \sqrt{(x_i - x_j)^2 + (y_i - y_j)^2}$  and  $D'_{i,j} = \sqrt{(x_i - x'_j)^2 + (y_i - y'_j)^2}$ .

A well-known analytical approximation of (2) is based on the concept of complex penetration depth, proposed by Deri *et al.*, which is adopted in a variety of industry-standard EMI analysis software [4], [5]. Let  $p$  be the complex depth, defined in meters as:

$$p = (1 - j) \frac{\delta}{2} = \sqrt{\frac{\rho}{j\omega\mu_0}}. \quad (3)$$

Then, under Deri's approach, the mutual impedance term described in (2) is simply written as [5]:

$$Z_m = j\omega \frac{\mu_0}{2\pi} \ln \left( \frac{\sqrt{(|y_i| + |y_j| + 2p)^2 + D^2}}{\sqrt{(|y_i| - |y_j|)^2 + D^2}} \right), \quad (4)$$

thus avoiding the need to explicitly perform the inverse Fourier transform expressed by the improper integral in (2), which is subjected to numerical instabilities due to the oscillating form of the integrand [6].

The issue is that real soils existing in nature are not uniform. Soils are reported to be layered media, frequently composed of three to five layers, and are deemed a recognized source of uncertainties in studies involving line impedances [7], [8]. Therefore, representing the soil as a uniform medium has the potential to introduce significant errors in the results, which may be unacceptable in studies of practical situations, when one is concerned with the safety of facilities and living beings.

Formal expressions for  $N$ -layered soil models have been derived by Nakagawa *et al.*, in terms of a convoluted recursive solution, with successive products of exponential terms on the integration variable  $\lambda$ , which requires specific numerical methods that are not always readily available in software commonly used in power systems and EMI analysis [9], [6].

To work around this difficulty and accurately model horizontally  $N$ -layered soils, described by respective permeabilities  $\mu_n$ , permittivities  $\epsilon_n$ , conductivities  $\sigma_n$  and thicknesses  $h_n$ , with  $n = 1, 2, \dots, N$ , the uniform variable  $\sigma$  in (2) is replaced by the equivalent parameter  $\sigma_{eq}$ , defined as in (5)-(7) [10]. The process is illustrated in Fig. 3.

This approach has been shown to provide accurate results within the frequency range from 60 Hz up to 1 MHz, with the advantage that a relatively simple expression is employed, yielding a single real-valued parameter that is fully compatible with any computational tool based in the original Carson equation (2), enabling the user to perform sophisticated simulations using resources already validated, peer-reviewed and widely available to the scientific community, as is the classic EMI circuit model described in the next section [2], [10], [11].

### B. Classic circuit model of the target line

Referring to Fig. 1, the circuit model classically used to determine induced voltages and currents on the target pipeline with parallel exposure to the energized conductor consists of representing the interfered system as the lossy transmission line section shown in Fig. 4, in which the voltage source  $E$  represents the mutual coupling with the energized conductor and is determined using (1) [2].

$$\sigma_{N-1,N} = \sigma_{N-1} \left[ \frac{(\sqrt{\sigma_{N-1}} + \sqrt{\sigma_N}) - (\sqrt{\sigma_{N-1}} - \sqrt{\sigma_N})e^{-2h_{N-1}\sqrt{\pi f \mu_{N-1} \sigma_{N-1}}}}{(\sqrt{\sigma_{N-1}} + \sqrt{\sigma_N}) + (\sqrt{\sigma_{N-1}} - \sqrt{\sigma_N})e^{-2h_{N-1}\sqrt{\pi f \mu_{N-1} \sigma_{N-1}}}} \right]^2, \quad (5)$$

$$\vdots$$

$$\sigma_{m-1,m} = \sigma_{m-1} \left[ \frac{(\sqrt{\sigma_{m-1}} + \sqrt{\sigma_{m-1,m}}) - (\sqrt{\sigma_{m-1}} - \sqrt{\sigma_{m-1,m}})e^{-2h_{m-1}\sqrt{\pi f \mu_{m-1} \sigma_{m-1}}}}{(\sqrt{\sigma_{m-1}} + \sqrt{\sigma_{m-1,m}}) + (\sqrt{\sigma_{m-1}} - \sqrt{\sigma_{m-1,m}})e^{-2h_{m-1}\sqrt{\pi f \mu_{m-1} \sigma_{m-1}}}} \right]^2, \quad (6)$$

$$\sigma_{eq} = \sigma_1 \left[ \frac{(\sqrt{\sigma_1} + \sqrt{\sigma_{m-1,m}}) - (\sqrt{\sigma_1} - \sqrt{\sigma_{m-1,m}})e^{-2h_1\sqrt{\pi f \mu_1 \sigma_1}}}{(\sqrt{\sigma_1} + \sqrt{\sigma_{m-1,m}}) + (\sqrt{\sigma_1} - \sqrt{\sigma_{m-1,m}})e^{-2h_1\sqrt{\pi f \mu_1 \sigma_1}}} \right]^2, \quad (1 \leq m \leq N-2). \quad (7)$$

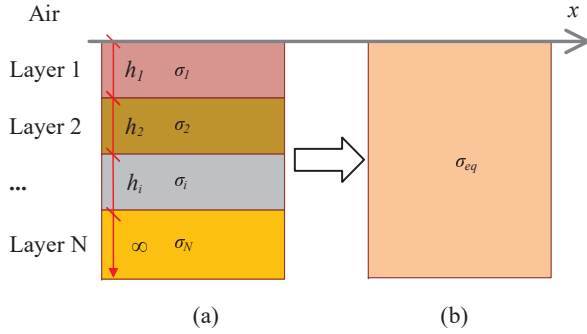
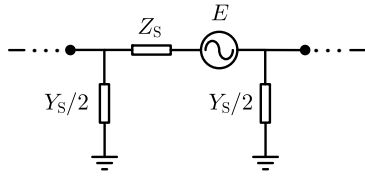

 Figure 3:  $N$ -layered soil model and uniform equivalent.


Figure 4: Equivalent circuit representing the target line shown in Fig. 1.

Impedance  $Z_S = Z_{S,int} + Z_{S,ext}$  represents the target line self-impedance and is composed by an internal part  $Z_{S,int}$ , which depends on the metal characteristics and geometry, and an external part  $Z_{S,ext}$ , related to the ground return path impedance. For a tubular conductor (a pipe) [2]:

$$Z_{S,int} = \frac{\sqrt{\rho_p \mu_0 \mu_p \omega}}{2\pi r_{ext} \sqrt{2}} (1 + j), \quad (8)$$

in which  $\rho_p$  is the conductor resistivity, in  $\Omega \cdot m$ ;  $\mu_p$  is the conductor relative permeability; and  $r_{ext}$  is the conductor outer radius, in meters. The external impedance component  $Z_{S,ext}$  is determined by setting  $j = i$ ,  $D_{i,i} = r_{ef}$ ,  $D'_{i,i} = 2|y_i|$  and  $D = 0$  in (2). The effective radius  $r_{ef}$  of the tubular conductor is determined according to the following relation [12]:

$$\ln(r_{ef}) = \ln(r_{ext}) - \frac{\frac{r_{ext}^4}{4} - r_{ext}^2 r_{int}^2 + r_{int}^4 \left[ \frac{3}{4} + \ln\left(\frac{r_{ext}}{r_{int}}\right) \right]}{(r_{ext}^2 - r_{int}^2)^2}, \quad (9)$$

in which  $r_{ext}$  and  $r_{int}$  are, respectively, the conductor external and internal radius, in meters.

Finally, the shunt admittance  $Y_S$  is given, for a coated tubular conductor, in S/m, as:

$$Y_S = \frac{2\pi r_{ext}}{\rho_c \delta_c} + j\omega \frac{\varepsilon_0 \varepsilon_c 2\pi r_{ext}}{\delta_c}, \quad (10)$$

in which  $r_{ext}$  is the conductor external radius, in meters;  $\rho_c$  is the coating specific resistivity, in  $\Omega \cdot m$ ;  $\delta_c$  is the coating thickness, in meters;  $\varepsilon_0$  is the vacuum electric permittivity, in F/m; and  $\varepsilon_c$  is the coating relative electric permittivity [2].

With the necessary parameters determined, complex interference geometries, composed of parallelisms, intersections and oblique approximations, are built by subdividing the target line in "equivalent parallelisms" and successively cascading the individual nominal- $\pi$  cells shown in Fig. 4 [2]. Then, induced voltages and currents follow from simple nodal analysis.

### III. CASE STUDY

#### A. System description

Fig. 5 represents a case study adapted from [1], with the side view shown in Fig. 6, which consists of a 25 kV single-phase overhead traction line (contact conductor) sharing the corridor with a 8" diameter underground steel pipeline with a depth-of-cover of 1.5 m.

The pipeline follows an oblique path in the vicinities of the railway, being modeled as one single equivalent parallel section with 1.5 km positioned 101 m apart from the traction line. This equivalent distance is calculated as the geometric mean of the vertex distances shown in Fig. 5, according to the procedure described in [2].

The contact conductor is made of stranded copper with a cross-section of 100 mm<sup>2</sup>, positioned at 5.5 m above the soil surface, operating with a maximum current of 600 A, 60 Hz, according to the technical data in [1]. Pipeline and coating material characteristics are given in Table I.

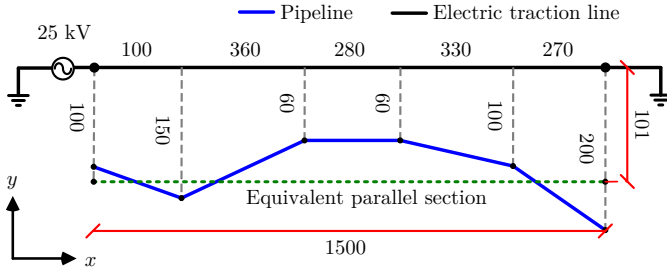


Figure 5: Approximation between an electric traction system and a pipeline. All distances in meters.

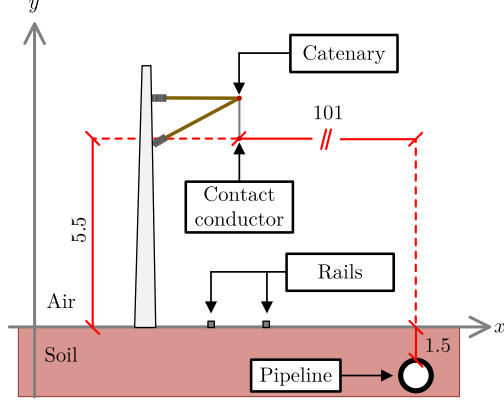


Figure 6: Single-phase traction line and pipeline side view. Dimensions in meters. Parallel length is 1.5 km.

Table I: Pipeline characteristics.

Parameter	Value
Internal radius [m]	0.1014
External radius [m]	0.1095
Electrical resistivity [ $\Omega \cdot \text{m}$ ]	$1.720 \times 10^{-7}$
Magnetic permeability [H/m]	$3.771 \times 10^{-4}$
Coating resistivity [ $\Omega \cdot \text{m}$ ]	$10^8$
Coating thickness [mm]	3

### B. Soil resistivity data

Soil parameters are determined from actual apparent resistivity measurements, which are performed according to the directions outlined in [13], with values shown in Table II.

By employing the estimation algorithm proposed in [14], it is found that the soil model that best adheres to the measured data is composed of six layers. The six-layered model parameters are computed using the least squares fitting method described in [15] and are presented in Table III and Fig. 7.

Using (5)-(7), and recalling that the resistivity  $\rho$  is the reciprocal of the conductivity  $\sigma$ , the uniform equivalent resistivity value that represents the six-layered model soil model is  $\rho_{eq} = 218.46 \Omega \cdot \text{m}$ , which corresponds to 51% of the apparent uniform value shown in Table II.

Table II: Apparent resistivity measurements.

Spacing [m]	Apparent resistivity [ $\Omega \cdot \text{m}$ ]
1	336.87
2	426.95
4	367.28
8	441.82
16	427.37
32	581.11
64	410.17
Uniform model	427.36

Table III: Parameters of the six-layered soil model.

Layer	$\rho$ [ $\Omega \cdot \text{m}$ ]	h [m]	Reflection	Contrast
1	267.10	0.20	-1.00	0.00
2	368.11	4.00	0.16	1.38
3	440.98	6.69	0.09	1.20
4	432.49	15.81	-0.01	0.98
5	578.44	26.31	0.14	1.34
6	205.09	$\infty$	-0.48	0.35

### C. Simulations

Simulations are performed to determine the voltages produced on the pipeline by the energized phase conductor due to inductive coupling, under different scenarios.

First, the finite element method is employed to compute voltages considering the actual system geometry with the six-layered soil structure given in Table III, using the FEMM software, which is a well known open-source finite element modeling and analysis tool that computes electromagnetic fields distribution over a meshed domain. Then, calculations are performed using the circuit model described in the preceding sections along with the uniform equivalent soil approach.

Fig. 8 shows the pipeline induced voltages due to the imperfect parallel exposure, considering the pipeline to be ungrounded (open circuit) at the extremities. Profiles show an excellent agreement between results produced by FEMM and the proposed technique, with a discrepancy of only 0.57%.

Voltages reach their maximum values at the pipeline extremities, which is consistent with the physics of the lossy

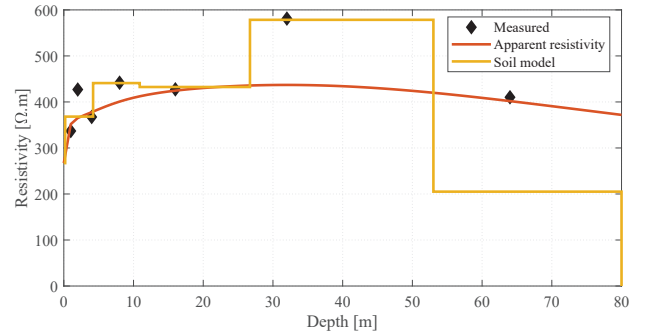


Figure 7: Computed and measured soil resistivities.

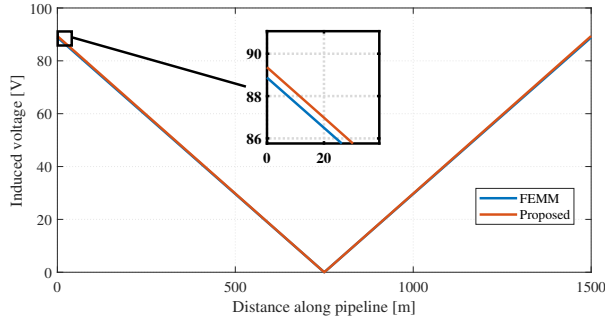


Figure 8: Pipeline induced voltages due to magnetic coupling with the phase conductor.

transmission line model represented in Fig. 4: if the pipeline is ungrounded, boundary conditions impose the current at its extremities to be zero. Therefore, voltages must be maximum, since the inducing current from the energized conductor is finite. Conversely, because of the same boundary condition and the symmetry of the equivalent parallel model, induced voltage is zero and induced current is maximum at the pipeline midpoint.

It is also relevant to observe the computational times involved: for the relatively simple parallel geometry studied, FEMM needed around 833 seconds ( $\sim 13$  minutes) to run calculations, whereas the circuit model required 3.51 seconds to be processed. Thus, the uniform equivalent formula combined with a circuit theory approach provides a performance gain of more than 99% in comparison with the finite element method, which is known to be a computationally expensive technique. This performance improvement is leveraged in the following discussion, in which variations of the original case are evaluated, in order to verify the soil influence on induced voltages.

Table IV and Fig. 9 illustrate the effect of soil resistivity on pipeline voltages. A total of eight additional simulations are carried out with the pipeline ungrounded and assuming the soil to be a semi-infinite homogeneous structure, with the apparent uniform value given in Table II, the resistivities given in Table III and the equivalent uniform value described in this work. Errors are relative to the FEMM (reference) response, which effectively accounts for the multilayered soil.

Results above show that the induced voltages increase with the soil resistivity. Moreover, the equivalent uniform approach, which emulates the soil multilayered property, yields results very similar to the case in which the soil is considered to be homogeneous with the resistivity equal to the bottom layer value. This indicates that the deepest soil layer is the one most affecting the inductive coupling response, which agrees with the soil model displayed in Fig. 3: the bottom layer is assumed to have an infinite thickness, thus it is expected to provide a more significant contribution to the impedance outcome.

The apparent uniform resistivity value is of the same order of magnitude of layers 2-5 and, in this case, may be con-

Table IV: Maximum voltages and errors with different resistivity scenarios.

Resistivity	Max. voltage [V]	Error [%]
Multilayered FEMM	88.87	0
Equivalent uniform	89.36	0.57
Apparent uniform	100.3	12.88
Layer 1 (top)	92.62	4.22
Layer 2	97.85	10.13
Layer 3	100.8	13.44
Layer 4	100.5	13.09
Layer 5	105.2	18.43
Layer 6 (bottom)	88.34	0.65

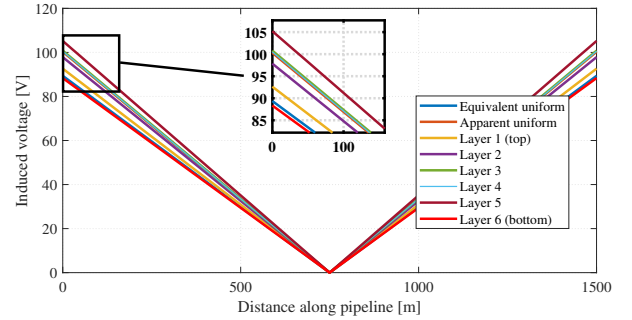


Figure 9: Induced voltages with uniform soil considering different resistivities.

sidered a reasonable conservative approximation of the actual soil behavior, with an error of 12% in the induced voltage. However, the assumption of a uniform soil model based on apparent resistivity readings should be handled very carefully, since the outcome is very sensitive to the statistical behavior of the measured samples. This could lead to grave mistakes in a situation which the first soil layers present low resistivity values, on top of a bottom layer with a high resistivity (for instance, wet soil layers above a large rocky layer). In this hypothetical case, measurements closer to the soil surface tend to decrease the arithmetic mean, when simulations show that the bottom layer (i.e. with the highest resistivity) will drive the resulting voltages to increased values.

#### IV. CONCLUSIONS

A case study of practical relevance to the industry was provided and discussed in this paper. Induced voltages on a pipeline due to a nearby energized conductor of a traction line over a six-layered soil were computed using finite element analysis and the classic circuit theory approach. The horizontally stratified soil structure was determined from actual field data and accounted by means of a homogenization technique which derives a uniform equivalent conductivity from  $N$ -layered soil parameters.

Results obtained using the proposed model agreed with the reference values under an error margin of only 0.57%, with a reduction of 99% in the computational times involved, and

emphasized the importance of properly accounting for the multilayered characteristic of real soils in problems involving ground return impedances.

Using a relatively simple equivalence formula, complex soil structures were introduced into a practical application using methods already available, tested and well-documented, with a relevant insight on how the deep soil layer affects the resulting voltages.

#### ACKNOWLEDGMENT

The authors gratefully acknowledge the support of PNPd/-CAPES.

#### REFERENCES

- [1] B. Milesevic, B. Filipovic-grcic, and T. Radosevic, "Electromagnetic Fields and Induced Voltages on Underground Pipeline in the Vicinity of AC Traction System," vol. 8, pp. 1333–1340, 2014.
- [2] CIGRÉ WG-36.02, "Technical Brochure n. 95 - Guide on the Influence of High Voltage AC Power Systems on Metallic Pipelines," Paris, pp. 1–135, 1995.
- [3] J. R. Carson, "Wave Propagation in Overhead Wires with Ground Return," *Bell Syst. Tech. J.*, vol. 5, pp. 539–554, 1926.
- [4] W. H. Dommel, "Digital Computer Solution of Electromagnetic Transients in Single- and Multiphase Networks," *IEEE Transactions on Power Apparatus and Systems*, no. 4, pp. 388–399, 1969.
- [5] A. Deri, G. Tevan, A. Semlyen, and A. Castanheira, "The Complex Ground Return Plane a Simplified Model for Homogeneous and Multi-Layer Earth Return," *IEEE Transactions on Power Apparatus and Systems*, vol. PAS-100, no. 8, pp. 3686–3693, aug 1981.
- [6] G. Papagiannis, D. Tsiamitros, D. Labridis, and P. Dokopoulos, "A Systematic Approach to the Evaluation of the Influence of Multilayered Earth on Overhead Power Transmission Lines," *IEEE Transactions on Power Delivery*, vol. 20, no. 4, pp. 2594–2601, oct 2005.
- [7] J. M. Whelan, B. Hanratty, and E. Morgan, "Earth Resistivity in Ireland," in *CDEGS Users' Group*. Montreal: Safe Engineering Services - SES, 2010, pp. 155–164.
- [8] S. Das, S. Santoso, A. Gaikwad, and M. Patel, "Impedance-based Fault Location in Transmission Networks: Theory and Application," *IEEE Access*, vol. 2, pp. 537–557, 2014.
- [9] M. Nakagawa, A. Ametani, and K. Iwamoto, "Further Studies on Wave Propagation in Overhead Lines with Earth Return: Impedance of Stratified Earth," *Proceedings of the Institution of Electrical Engineers*, vol. 120, no. 12, p. 1521, 1973.
- [10] A. G. Martins-Britto, F. Lopes, and S. Rondineau, "Multi-layer Earth Structure Approximation by a Homogeneous Conductivity Soil for Ground Return Impedance Calculations," *IEEE Transactions on Power Delivery*, vol. 35, no. 2, pp. 881–891, 2020.
- [11] A. G. Martins-Britto, "Realistic Modeling of Power Lines for Transient Electromagnetic Studies," Doctoral Thesis, University of Brasília, 2020.
- [12] H. L. Seneff, "Study of the Method of Geometric Mean Distances Used in Inductance Calculations," 1947.
- [13] IEEE, "Guide for Measuring Earth Resistivity, Ground Impedance, and Earth Surface Potentials of a Ground System," New York, NY, p. 54, 1984.
- [14] B. Zhang, X. Cui, L. Li, and J. He, "Parameter Estimation of Horizontal Multilayer Earth by Complex Image Method," *IEEE Transactions on Power Delivery*, vol. 20, no. 2 II, pp. 1394–1401, 2005.
- [15] T. Takahashi and T. Kawase, "Analysis of Apparent Resistivity in a Multi-Layer Earth Structure," *IEEE Transactions on Power Delivery*, vol. 5, no. 2, pp. 604–612, 1990.